Upregulation of α-synuclein during localized radiation therapy signals the association of cancer-related fatigue with the activation of inflammatory and neuroprotective pathways

LN Saligan[1,*], **CP Hsiao**[1], **D Wang**[1], **XM Wang**[1], **L St. John**[1], **A Kaushal**[2], **D Citrin**[2], **JJ Barb**[3], **PJ Munson**[3], and **RA Dionne**[1]

[1]National Institute of Nursing Research, National Institutes of Health, Bethesda, Maryland, USA

[2]National Cancer Institute, National Institutes of Health, Bethesda, Maryland, USA

[3]Center of Informational Technology, National Institutes of Health, Bethesda, Maryland, USA

Abstract

Purpose—Neuroinflammatory mechanisms are associated with fatigue in neurodegenerative conditions such as Parkinson's. The symptoms in Parkinson's including fatigue are thought to be related to α-synuclein overexpression. This study investigated genomic correlates of fatigue experienced by men with prostate cancer receiving external beam radiation therapy (EBRT).

Patients and Methods—Sixteen men with non-metastatic prostate cancer who were scheduled to receive EBRT were enrolled. Fatigue scores and blood were obtained at baseline (prior to EBRT, D0); one hour following initiation of EBRT (D1), day 7 (D7), day 14 (D14), midpoint (days 19–21, D21), completion (days 38–42, D42), and four weeks post EBRT (days 68–72, D72). Gene expression profiling using microarray analysis was performed from whole blood and confirmatory qPCR and protein (ELISA) analyses verified the microarray results. Correlations between fatigue and gene/protein expressions were determined using a mixed model approach.

Results—Microarray data showed significant, differential expression of 463 probesets following EBRT. *SNCA* had a 2.95 fold change at D21 from baseline. *SNCA* expression was confirmed by qPCR ($p < 0.001$) and ELISA ($p < 0.001$) over time during EBRT. Fatigue scores were significantly correlated with *SNCA* gene expression on D14 ($r = 0.55$, $p < 0.05$) and plasma α-synuclein concentrations on D42 of EBRT ($r = 0.54$, $p = 0.04$).

Conclusion—Fatigue experienced during EBRT may be mediated by α-synuclein overexpression. Alpha-synuclein may serve as a useful biomarker to understand the mechanisms and pathways related to the development of fatigue in this population.

Localized radiation therapy is one of the main therapeutic options recommended for the management of non-metastatic prostate cancer (Thompson et al., 2007). Advances in prostate cancer treatment using improved techniques in the delivery of localized therapy such as external beam radiation therapy (EBRT) have led to high cure rates and prolonged the natural history of the disease. However, the improved survival rates are mitigated by the

Corresponding Author: Leorey N. Saligan, PhD, RN, CRNP, National Institute of Nursing Research, National Institutes of Health, 9000 Rockville Pike, Building 10, Room 2-1339, Bethesda, MD 20892, Phone: 301-451-1685 Fax: 301-480-1413, saliganl@mail.nih.gov.

toxicities associated with these treatments that lower the quality of life for survivors. Fatigue is one of the most commonly reported and the most distressing side effect reported in the radiation therapy setting, affecting approximately 78% (range = 31%–100%) of patients receiving localized radiation therapy (Greenberg et al., 1992; Smets et al., 1998). It is also the most common baseline symptom noted in men with prostate cancer referred for a curative course of radiation therapy (Danjoux et al., 2007) and one of the major indicators of cancer therapeutic outcomes (Monga et al., 1999). Fatigue severity of most men with prostate cancer is known to increase significantly during the and declining after completion of therapy course of radiation therapy peaking at midpoint (Miaskowski et al., 2008). The etiology of fatigue progression and severity while receiving cancer treatment is currently unknown. However, neuroinflammation has been reported to be related to fatigue in other conditions (Bokemeyer et al., 2011; Rönnbäck & Hansson, 2004).

Although the National Comprehensive Cancer Network (NCCN) practice guidelines recommend the use of methylphenidate as a pharmacological intervention for cancer-related fatigue (CRF) (Mock et al., 2000) based on evidence from small, single arm trials (Bruera et al., 2003; Hanna et al., 2006), randomized clinical studies failed to validate these results (Bruera et al., 2006; Butler et al., 2007; Mar Fan et al., 2008). There is currently no optimal pharmacologic therapy and scant molecular evidence to guide the development of effective therapies for the management of cancer- and/or cancer treatment-related fatigue. This hypothesis-generating study explored genomic correlates of cancer-related fatigue by investigating changes in gene expression specifically focusing on those genes that are associated with neuroinflammation and their relationship with fatigue scores during EBRT. This approach may assist in understanding the contribution of neuroinflammation in the development of cancer-related fatigue and may provide new insights for potential interventional targets. This study uses an unbiased approach to demonstrate the associations between differential gene expression changes from whole blood and fatigue scores over time during EBRT.

Methods

Men with non-metastatic prostate cancer were enrolled under an actively recruiting protocol 09-NR-0088 (NCT00852111). Data collection was conducted from May 2009 to December 2010. Study outcomes were measured at baseline (prior to EBRT, D0); one hour following initiation of EBRT (D1), day 7 (D7), day 14 (D14), at midpoint (days 19–21, D21), at completion (days 38–42, D42), and four weeks post EBRT (days 68–72, D72). Patients with progressive disease causing significant fatigue; psychiatric disorder within five years; uncorrected hypothyroidism or anemia; taking sedatives, steroids, or non-steroidal anti-inflammatory agents; or second malignancies were excluded. Fatigue was measured at each time point using the revised Piper Fatigue Scale (rPFS), a 22-item paper/pencil questionnaire that has a zero to ten rating scale (0 = none; 10 = worst intensity) and defines severe fatigue as a score of > 6 (Piper et al., 1998). Only subjects with rPFS scores and corresponding quantitative real-time polymerase chain reaction (qPCR) data were included in the final analysis. Depressive symptoms were also assessed at each time point using the clinician-administered, 21-item Hamilton Depression Rating Scale (HAM-D), which has been validated in other fatigue studies (Lydiatt et al., 2008).

Blood for gene expression, responses to fatigue and depression questionnaires were also obtained during one outpatient visit from age, gender, and race-matched healthy controls enrolled under protocol 09-NR-0131 (NCT00888563). Data from these healthy volunteers were used to compare baseline (D0) data obtained from study subjects in order to establish that study subjects are similar to healthy individuals prior to EBRT. Exclusion criteria for healthy controls were: confirmed medical condition causing clinically significant fatigue;

taking medications known to cause fatigue; worked late evening and night shifts within the past month; reported a severe psychiatric condition; consuming > 300 mg of caffeine-containing beverages or > 1 lb of chocolate a day; consuming > 2 servings of alcohol-containing beverages everyday; and having detectable blood alcohol content. Both protocols were approved by the Institutional Review Board of the National Institutes of Health (NIH), Bethesda, Maryland, USA.

Gene expression chip processing and pathway analysis

For an unbiased, hypothesis-generating approach, several steps were chronologically followed in the study. First, an initial gene expression profile was explored using microarray technology to determine a list of differentially expressed genes during EBRT. At each time point, 2.5 mL of blood from subjects was collected using RNA PAXGene tubes (Qiagen, Frederick, Maryland) for each of the seven time points. The collected blood was stored at $-80°C$ in a freezer until ready for RNA extraction. RNA extraction, purification, cDNA and cRNA synthesis, amplication, hybridization, scanning and data analyses were conducted following standard protocols as previously described (Wang et al., 2007). A total of 80 Affymetrix microarray chips (HG U133 Plus 2.0, Santa Clara, California) were used for gene expression analysis. Affymetrix GeneChip Command Console (AGCC, 3.0 V) was used to scan the images for data acquisition. Raw signal intensity values were normalized using S10 transformation algorithm from the MSCL Analyst's Toolbox. S10 transformation is a variance stabilizing, quantile normalization transform and is scaled to match a base 10 logarithm. S10 values were subjected to principal component analysis in order to detect outliers. Seven chips were identified as outliers and excluded from further analysis. The remaining transformed data were subjected to linear regression analysis adjusted for patient effect with respect to the seven time points treated as equal intervals. The slope measured the trend of expression change between baseline through D72.

Ingenuity Pathway analysis (Ingenuity® Systems, www.ingenuity.com, Redwood City, California) identified functional networks of the differentially expressed probesets from the Ingenuity's Knowledge Base. Right-tailed Fisher's exact test was used to calculate p-values determining the probability that each biological function and/or disease assigned to these networks was due to chance alone.

Confirmatory Quantitative Real Time Polymerase Chain Reaction (qPCR)

Second, in order to confirm the differentially expressed genes in the microarray experiment, qPCR was performed from the same RNAs used in the microarray experiment in all seven time points for the study subjects and at one study time point for the matched controls. Total RNA was isolated with an RNA kit and treated with DNase I during purification. First strand cDNAs were synthesized using RT^2 First Strand Kit (Qiagen, Frederick, Maryland) with 100 ng of total RNA from each sample and subsequently diluted tenfold with dH_2O. The qPCR amplification mixers (10 μl) contained one μl of diluted first strand cDNA, five μl of 2X RT^2 Real Time SYBR Green/Rox PCR Master Mix (Qiagen, Frederick, Maryland) and 400 nM of forward and reverse primers. Reactions were carried on ABI PRISM 7900HT Sequence Detection System and were subjected to initial ten minute denaturation at 95°C and 40 cycles at 95°C for 15 seconds and 60°C for 60 seconds.

Five potential reference genes were tested including *B2M* (beta-2-microglobulin)*, HPRT1* (hypoxanthine phosphoribosyltransferase 1)*, RPL13A* (ribosomal protein L 13a)*, GAPDH* (glyceraldehydes-3-phosphate dehydrogenase) and *ACTB* (actin, beta). *GAPDH* and *ACTB* were validated and chosen as reference genes. Primers of *GAPDH* (reference position 1287), *ACTB* (reference position 1222) and SNCA (reference position 876) (Qiagen, Frederick,

Maryland) had efficiencies between 90% and 110%. When calculating for ΔCt values, geometric means of Ct values of the 2 reference genes were used.

Confirmation by ELISA

Third, protein levels from plasma separated from whole blood collected from the same patients in the microarray experiment using EDTA tubes in all seven time points and stored at −80° C were quantified using human protein ELISA kits (Invitrogen, Camarillo, California). ELISA was performed using 50 μl of plasma samples according to manufacturer's guide. The plates were read in a microplate reader VICTOR3 at 450 nm. All samples were tested in triplicate.

Supporting test

Cultured prostate tumor cells (GUMC-30) from Georgetown University, School of Medicine, Department of Pathology, were used to confirm *in vitro* gene expressions pre- and post-irradiation of primary prostate tumor cells, using qPCR and ELISA. Two sets of GUMC-30 cells were exposed to two doses of gamma-ray irradiation (1 Gy and 2 Gy). RNA and protein were extracted from GUMC-30 cells at 4 and 24 hours post irradiation. The total RNAs were dissolved in 1 ml Trizol and extracted using a modified guanidine thiocyanate-phenol/chloroform method, treated with RNase-free DNase to remove residual DNA, precisely quantified, and stored at −80°C for qPCR analysis. Beta-actin was used as the endogenous control. ACTB was used as the endogenous control. Cell lysates were extracted using RIPA buffer according to instructions provided by ELISA kit (Invitrogen, Grand Island, NY). Protein expression from both irradiated and non-irradiated GUMC-30 cells were measured by ELISA at both time points (4 and 24 hours post irradiation).

Statistical Methods

Descriptive statistics were calculated for the participants' demographic characteristics. Linear regression, linear mixed effect models using patient as a random effect and the study time points as the fixed effect, and correlation analyses were conducted between the microarray data and fatigue scores using the JMP Statistical Discovery software™ and a package of scripts (MSCL Toolbox, http://abs.cit.nih.gov/MSCLToolbox) developed by two of the authors of this paper (JJB, PJM). Independent t-tests were used to compare the mean differences of fatigue, gene and protein expressions from subjects at D0 and matched controls, and between baseline (D0) data and data from later time points during EBRT. Repeated measures ANOVA was used to determine how variables change over time during EBRT compared to baseline data.

Correlations between fatigue and gene/protein expressions were determined using a mixed model approach. Mixed model analyses for the individual growth curve analysis for fatigue scores and gene/protein results were carried out to estimate the intercept and slope of the individual growth curve of each of these variables. The time variables were entered in the models in terms of days in EBRT. A simple linear relationship was assumed in the time variable. The intercepts and slopes of the outcome variable (fatigue) and the most important clinical predictor (gene or protein expressions) for each participating individual were estimated in the mixed model. In the analyses, we modeled the changes over time in a linear fashion. The intercept of the individual growth curve represents the estimated baseline (D0) value for each patient based on a linear trajectory of the fatigue scores over time (in terms of EBRT days). The slope of the individual growth curve represents the estimated rate of change over time during EBRT for each patient based on a linear trajectory of their fatigue scores. The intercepts and slopes of fatigue scores and clinical predictors (gene and protein expressions) were estimated based on a mixed model for each patient and the resulting

estimated intercepts and slopes were then correlated. No replacement values were assigned for missing data.

Results

To obtain an initial list of candidate genes, a gene expression profile from peripheral blood of nine subjects collected during EBRT was initially conducted using microarray analysis at seven time points (D0, D1, D7, D14, D21, D42, D72). Four hundred sixty three probesets (178 upregulated and 285 down regulated) were differentially expressed over time after the probesets passed filtering criteria of 1% false discovery rate (FDR) and a slope of 0.07 or more (over 2.6-fold change, $p < 0.001$). The most differentially expressed genes were related to inflammation (interferon alpha-inducible protein 27 [*IFI27*], B-lymphocyte antigen CD20 [*MS4A1*], Ig mu chain C region [*IGHM*], C-C chemokine receptor type 7 [CCR7]), and iron synthesis (carbonic anhydrase 1 [*CA1*], hemoglobin subunit delta [*HBD*], hemoglobin subunit gamma-2 [*HBG2*], alpha hemoglobin stabilizing protein [*AHSP*], iron-sulfur cluster assembly 1 homolog [*ISCA1*]). Table 1 shows the expression values of the top 20 genes that were differentially expressed in the microarray experiment, which included *SNCA,* the gene encoding α-synuclein. Because *SNCA* has been associated with neuroinflammation (Gao et al., 2011), it was selected for further investigation in this study. The *SNCA* gene had a 2.95-fold change in expression at D21 compared to baseline or an expression value of 0.47 on a log 10 scale. The average log 10 expression over five *SNCA* probesets over patients was plotted over time during EBRT (Figure 1), where a significant upward trend of *SNCA* expression was noted ($p < 0.0001$). The canonical pathways related to *SNCA* overexpression during EBRT using Ingenuity® revealed pathways related to 14-3-3-mediated signaling, which is involved in phosphorylation-dependent protein-protein interactions (Wilker & Yaffe, 2004).

Confirmation of SNCA expression during EBRT

A qPCR was performed to confirm the expression of *SNCA* on the same RNAs extracted from peripheral blood of nine subjects in the microarray experiment and RNAs from an additional seven patients who received EBRT at the same seven time points (N = 9 + 7 = 16). *SNCA* expression (ΔCt value) was also measured from whole blood cell RNAs collected at one time point from matched controls. Both *GAPDH* and *ACTB* genes were used as reference genes. There was no significant difference between the baseline (pre-EBRT) values of the 16 subjects and 16 matched controls ($p = 0.83$). There was a significant change in *SNCA* expression at each time point during EBRT and even in D72 compared to baseline ($p \quad 0.009$). Repeated measures ANOVA showed a significant change of *SNCA* expression from D0 and over time during EBRT as measured by qPCR (Wilks' lambda = 0.09, F(6,10) = 16.00, $p < 0.01$, Figure 2).

Further confirmatory protein analyses of *SNCA* expression was performed on plasma samples collected at all seven time points from the same patients used in the qPCR experiment. Two of the 16 patients used in the qPCR experiment had missing α-synuclein plasma concentrations, so 14 subjects were included in the analyses. The plasma concentrations of α-synuclein decreased from baseline to D21, and increased from D21 to D72 (Figure 3). Compared to the baseline data, there was a significant change in plasma α-synuclein concentration on D7 ($p = 0.04$), D14 ($p = 0.03$), and D21 ($p = 0.008$) of EBRT using independent t-tests. Repeated measures ANOVA showed a significant change of α-synuclein plasma concentrations over time (Wilks' Lambda = 0.178, F (6,8) = 6.14, $p = 0.01$) during EBRT compared to D0.

The correlation of *SNCA* expression intercept and plasma α-synuclein concentration intercept was negative and significant using the mixed model approach ($r = -0.69$, $p =$

0.006), suggesting that higher baseline plasma α-synuclein concentration is related to smaller baseline *SNCA* expression. This is a consistent confirmatory result because higher ΔCt values from the qPCR data reflect lower *SNCA* expression, therefore this result confirmed that low baseline *SNCA* and α-synuclein expressions are significantly associated. The correlation of *SNCA* expression intercept and plasma α-synuclein concentration slope was significant ($r = 0.67$, $p = 0.008$), suggesting that the higher the estimated baseline ΔCt *SNCA* expression, the larger the estimated rate of change for the plasma α-synuclein concentration during EBRT. The negative correlation between *SNCA* expression slope and plasma α-synuclein concentration slope was significant ($r = -0.61$, $p = 0.02$), suggesting that large estimated rate of change of *SNCA* expression is related to a small estimated rate of change of plasma α-synuclein concentration during EBRT.

Fatigue during EBRT

The baseline (D0) fatigue scores of 16 subjects were not significantly different from matched controls ($p = 0.22$). Compared to the baseline fatigue scores (mean = 1.6 ± 1.6), the mean fatigue scores significantly increased at midpoint (D21) of EBRT (mean = 2.9 ± 2.0, $p = 0.003$), continued to be significantly higher at completion (D42) of treatment (mean = 2.7 ± 2.3, $p = 0.007$), but showed no significant difference one month post-EBRT (mean = 2.5 ± 2.5, $p = 0.10$, Figure 4). Repeated measures ANOVA of fatigue scores showed that the assumption of sphericity was violated and the Wild's Lambda with adjusted degree of freedom as the lower bound was significant. It indicated that the change of fatigue symptoms over time was close to the significance level, depending on the adjustment used. The type III Sum of Squares = 24.80, and with the lower-bound adjusted degree of freedom, $F (1, 15) = 3.40$, $p = 0.09$. The Wilk's Lambda = 0.29, $F (6, 10) = 4.04$, $p = 0.03$. With the adjusted Huynh-Feldt degree of freedom, the $F (4.0, 59.98) = 3.40$, $p = 0.01$. Findings indicate a trend for fatigue scores to change over time until D42 of EBRT.

Correlation between fatigue scores and α-synuclein expression

Correlations using independent t-tests between *SNCA* expressions measured by qPCR and fatigue scores suggest that EBRT produces the same effects on fatigue and *SNCA* expression. The correlations between the two variables were large and consistent during EBRT especially in time points D7 ($r = 0.60$, $p < 0.05$), D14 ($r = 0.55$, $p < 0.05$), and D21 ($r = 0.62$, $p < 0.05$). Using a mixed model approach, the correlation of *SNCA* qPCR expression intercept and fatigue intercept trended towards significance ($r = 0.50$, $p = 0.06$, Figure 5a). The fatigue slope was not correlated with *SNCA* qPCR expression slope ($p = 0.84$, Figure 5b), suggesting that the two values may be fairly close in level within individual patients, but the rates at which they change over time during EBRT were not closely related.

A significant correlation in D42 between fatigue scores and plasma α-synuclein concentrations was noted using independent t-tests ($r = 0.54$, $p = 0.04$). The correlation of plasma α-synuclein concentration intercept and fatigue intercept was significant using the mixed model approach ($r = -0.60$, $p = 0.03$, Figure 5c), suggesting that larger baseline plasma α-synuclein concentrations were associated with smaller baseline fatigue scores. The correlation of fatigue intercept and plasma α-synuclein concentration slope was significant ($r = 0.76$, $p = 0.002$, Figure 5d), suggesting that as the fatigue intercept increased, the plasma α-synuclein concentration slope increased. It means that if the estimated baseline value of a patient's fatigue score was high, the rate of change of plasma α-synuclein concentration during EBRT was also high.

Demographic characteristics of subjects

A total of 16 patients with complete fatigue and qPCR data were included in the analyses. Sixteen age-, gender-, and race- matched healthy controls with no prostate cancer were used

as controls to compare baseline gene expression and fatigue scores of study participants. Table 2 describes the demographic and clinical characteristics of the study participants. The mean age of all participants was 63.2 years (± 8.5), which is within ± 5 years from the matched controls (58.5 ± 10.8). Five of the 16 participants had T2a clinical T-stage of their prostate cancer, two had a T1c stage, and the rest had a T2b to T3c stage (N = 9/16) (Campbell et al., 2001). Six patients (38%) had a Gleason score of 9 and 10 patients had Gleason scores between 6 and 8. At baseline, 15 participants had a score of 90 on the Karnofsky Performance Scale indicating that they were able to carry out normal activities with minor signs or symptoms of disease. Fourteen patients (88%) received androgen deprivation therapy two months before EBRT and three patients had radical prostatectomy more than 6 months before receiving EBRT. At baseline, testosterone levels ranged from 20 to 505 ng/dL with a mean of 211.3 ng/dL (normal = 181.0–758.0 ng/dL). Thyroid stimulating hormone (TSH) (range = 0.24–3.84 mcIU/mL; normal = 0.4–4.0 mcIU/mL) and albumin levels were normal (range = 3.5–4.5 g/dL; normal = 3.7–4.7 g/dL). Baseline PSA levels (mean = 21.0 ± 27.6) decreased post-EBRT (mean = 0.1 ± 0.3) and hematocrit levels, which were normal at baseline (mean = 40.9 ± 3.4; normal = 40.1–51.0%) decreased at completion of EBRT (mean = 37.8 ± 2.8). None of the patients reached the cutoff score for depression using the Hamilton Depression Scale (HAM-D) at baseline (mean = 1.4 ± 2.5) nor at completion of EBRT (mean = 2.0 ± 2.7). Eighty eight percent (N = 14/16) of patients received a total dose of 75.6 Gray with IMRT, while the remaining 2/16 received a total dose of 68.4 Gray.

Supporting tests

A subset of this investigation was to confirm whether upregulation of *SNCA* is observed in the primary prostate tumor tissue at different time points with increasing dose of radiation. Primary prostate tumor cells (GUMC-30), a generous donation from Dr. Hang Yuan and Dr. Richard Schlegel of the Georgetown University, School of Medicine, Department of Pathology, were exposed to 1 Gy and 2 Gy doses of radiation. Compared to pre-radiation expression, which is serving as the control, there was not a significant increase of qPCR *SNCA* expression post radiation using both doses using ΔCt ($p > 0.62$). There was not a significant change in *SNCA* expression between the two time points (4 and 24 hours) using 2 Gy radiation ($p = 0.15$), but a significant decrease in *SNCA* expression (ΔCt) was observed from 4 to 24 hours after exposure to 1 Gy radiation ($p = 0.01$), indicating that time-related effect of radiation to *SNCA* expression is better observed using 1Gy dose. Compared to non-irradiated cells, α-synuclein protein concentration measured by ELISA from GUMC-30 cell lysates increased > 30% at four hours and > 70% at 24 hours after receiving 2 doses (1 Gy and 2 Gy) of radiation (Figure 6).

Discussion

To our knowledge, this study is the first to demonstrate that a differential expression of a novel gene related to neuroinflammation is significantly associated with changes in fatigue symptoms of men with non-metastatic prostate cancer receiving localized radiation therapy. Alpha-synuclein is reported to have an important physiologic role in neurotransmission by serving as an activity-dependent inhibitor during synaptic transmission; however, α-synuclein can form toxic oligomers that could promote cellular damage and degeneration in pathologic states (Sulzer, 2010). In pathologic states, α-synuclein is known to form inclusions in dopaminergic and non-dopaminergic neurons (Musgrove et al., 2011). Alpha-synuclein is known to cause mitochondrial impairments and cellular damage enhancing cellular oxidative stress (Hsu et al., 2000), which can lead to neurodegeneration (Hashimoto et al., 1999), as seen in dementia, Parkinsonism, and other behavioral impairments (Olivares et al., 2009).

As part of a physiologic response to intrinsic or external stressors, α-synuclein is expressed to serve as a neuroprotective mechanism against subsequent insults (Musgrove et al., 2011), which might explain its overexpression in this study. In physiologic states, previous studies confirm that an elevated level of the α-synuclein protein in cellular cytoplasm is a measure of resilience against oxidative stress and cellular protection from toxic insults (Hashimoto et al., 2002; Manning-Bog et al., 2003; Monti et al., 2007). Alpha-synuclein is observed as a molecular chaperone to many physiologic proteins such as the muscarinic receptors (Leng, Chase, and Bennett, 2001), and the SNARE proteins (Burre et al., 2010). The findings of this study seem to suggest that overexpression of α-synuclein from an acute insult induces worsening of fatigue symptoms through its physiologic neuroprotective role, which is maintaining neuronal catecholamine homeostasis as reported by Goldstein (2011). Overexpression of α-synuclein has been found to cause specific physiological impairment of neuronal catecholamine release (Nemani et al., 2010). Furthermore, metabolic insults posed by the radiation therapy on mitochondrial function, can lead to retardation of energy-requiring processes such as neuronal uptake and vesicular sequestration of catecholamines (Goldstein, 2011). The impairment in neuronal catecholamine release can lead to dysfunctional sympathetic and parasympathetic responses, which have been observed in fatigued cancer survivors (Fagundes et al., 2011). The disarray in sympathetic and parasympathetic responses can also activate the proinflammatory cytokine network (Fagundes et al., 2011). High levels of pro-inflammatory cytokines (IL-6, IL-1β) (Wratten et al., 2004; Bower et al., 2007) and activated immune cells (CD4+ T lymphocytes) have been observed in individuals reporting fatigue while receiving cancer therapy (Bower et al., 2007).

The overexpression of the *SNCA* gene observed in this study indicates that neuroinflammatory mechanisms may play a role in the development of fatigue in this population, considering α-synuclein's role in neuroprotection (Musgrove et al., 2011). Markers of neuroinflammation, as evidenced by high levels of brain metabolites (choline, creatine, inositol) were reported in fatigued hepatitis C-positive individuals with mild liver disease using magnetic resonance spectroscopy (Bokemeyer et al., 2011). Increased levels of these brain metabolites are thought to cause microglial activation and induce pro-inflammatory cytokine release (Grover et al., 2012). Establishing the role of neuroinflammation in fatigue development using genomic approaches or through brain imaging is a step forward in understanding mechanisms of fatigue. It is also important to identify molecular activators and inhibitors of *SNCA* expression using cell-based assays in order to understand associated pathways that may contribute to fatigue development.

There was a decline in α-synuclein protein concentration observed in this study, especially after initiation of EBRT until midpoint of the treatment, which was not observed in the *SNCA* gene expression. Previous studies also observed similar dissociation in α-synuclein gene and protein expressions, which was attributed to many factors including alterations in genetic variations in *SNCA* alleles (Linnertz et al., 2009; Westerlund et al., 2008). Aging has also been associated with the dissociation of α-synuclein gene and protein expressions, where α-synuclein protein concentration increased with age, independent of mRNA levels (Li et al., 2004). A recent study suggested that the dissociation in α-synuclein gene and protein expressions may result from a number of mechanisms including reduction in mRNA translation, increased clearance of α-synuclein turnover, or sequestration of α-synuclein into an insoluble form (Quinn et al., 2012). Further investigation is necessary to explain the differences in α-synuclein gene and protein expressions observed in this study including the analysis of age group differences that may exist in the levels of soluble α-synuclein proteins.

Although the study findings do not directly support the concept that *SNCA* causes the development of fatigue associated with cancer or its treatment, they stimulate important

questions that warrant further investigation to understand the role of specific mechanisms such as neuroinflammation in the development of fatigue. The current study is limited by having only explored the association between α-synuclein and fatigue, further investigation is necessary to explore the role of other networks involved in fatigue development such as inflammation and iron-synthesis because genes related to these networks were observed to be differentially expressed in this study. There is currently no optimal management for CRF because its etiology is not understood. A recent comprehensive review of the state of the science of CRF revealed that several interventional studies have reported contradictory results in reducing CRF (Mitchell, 2010). The findings reported in this study suggest that fatigue associated with α-synuclein overexpression may provide mechanistic insight to the etiology of CRF and novel interventions for its clinical management.

Conclusion

Without knowing the molecular-genetic etiology of CRF, interventional options to manage CRF will remain challenging. Identification of possible biomarkers for CRF may provide insight on possible therapeutic targets to manage CRF. Determining the functional significance of the association between fatigue symptoms and α-synuclein expression may also identify other key nodal pathways, such as neuroinflammation, which may help explain the mechanisms behind CRF. Replication of these findings in populations with other types of cancer and those receiving other types of cancer treatments is important to pursue to determine whether the candidate genes reported in this study are also differentially expressed when fatigue develops in those populations.

References

Bokemeyer M, Ding XQ, Goldbecker A, Raab P, Heeren M, Arvanitis D, et al. Evidence for neuroinflammation and neuroprotection in HCV infection-associated encephalopathy. Gut. 2011; 60:370–377. [PubMed: 20926642]

Bower J, Ganz P, Aziz N, Olmstead R, Irwin MR, Cole SW. Inflammatory responses to psychological stress in fatigued breast cancer survivors: relationship to glucocorticoids. Brain Behav Immun. 2007; 21:251–258. [PubMed: 17008048]

Bruera E, Driver L, Barnes EA, Willey J, Shen L, Palmer JL, et al. Patient-controlled methylphenidate for the management of fatigue in patients with advanced cancer: a preliminary report. J Clin Oncol. 2003; 21:4439–4443. [PubMed: 14645434]

Bruera E, Valero V, Driver L, Shen L, Willey J, Zhang T, et al. Patient-controlled methylphenidate for cancer fatigue: a double-blind, randomized, placebo-controlled trial. J Clin Oncol. 2006; 24:2073–2078. [PubMed: 16648508]

Burre J, Sharma M, Tsetsenis T, Buchman V, Etherton MR, Sudhoff TC. Alpha-synuclein promotes SNARE-complex assembly in vivo and in vitro. Science. 2010; 329:1663–1667. [PubMed: 20798282]

Butler JM Jr, Case LD, Atkins J, Frizzell B, Sanders G, Griffin P, et al. A phase III, double-blind, placebo-controlled prospective randomized clinical trial of d-threo-methylphenidate HCl in brain tumor patients receiving radiation therapy. Int J Radiat Oncol Biol Phys. 2007; 69:1496–1501. [PubMed: 17869448]

Campbell T, Blasko J, Crawford ED, Forman J, Hanks G, Kuban D, et al. Clinical staging of prostate cancer: reproducibility and clarification of issues. Int J Cancer. 2001; 96:198–209. [PubMed: 11410889]

Danjoux C, Gardner S, Fitch M. Prospective evaluation of fatigue during a course of curative radiotherapy for localised prostate cancer. Support Care Cancer. 2007; 15:1169–1176. [PubMed: 17333296]

Fagundes CP, Murray DM, Hwang BS, Gouin JP, Thayer JF, Sollers JJ, et al. Sympathetic and parasympathetic activity in cancer-related fatigue: more evidence for a physiological substrate in cancer survivors. Psychoneuroendocrinology. 2011; 36:1137–1147. [PubMed: 21388744]

Gao HM, Zhang F, Zhou H, Kam W, Wilson B, Hong JS. Neuroinflammation and α-synuclein dysfunction potentiate each other, driving chronic progression of neurodegeneration in a mouse model of Parkinson's disease. Environ Health Perspect. 2011; 119:807–814. [PubMed: 21245015]

Goldstein D. Stress, allostatic load, catecholamines, and other neurotransmitters in neurodegenerative diseases. Endocr Regul. 2011; 45:91–98. [PubMed: 21615193]

Greenberg DB, Sawicka J, Eisenthal S, Ross D. Fatigue syndrome due to localized radiation. J Pain Symptom Manage. 1992; 7:38–45. [PubMed: 1538180]

Grover VP, Pavese N, Koh SB, Wylezinska M, Saxby BK, Gerhard A, et al. Cerebral microglial activation in patients with hepatitis c: in vivo evidence of neuroinflammation. J Viral Hepat. 2012; 19:e89–96. [PubMed: 22239531]

Hanna A, Sledge G, Mayer ML, Hanna N, Einhorn L, Monahan P, et al. A phase II study of methylphenidate for the treatment of fatigue. Support. Care Cancer. 2006; 14:210–215.

Hashimoto M, Hsu LJ, Rockenstein E, Takenouchi T, Mallory M, Masliah E. Alpha-synuclein protects against oxidative stress via inactivation of the c-Jun N-terminal kinase stress-signaling pathway in neuronal cells. J Biol Chem. 2002; 277:11465–11472. [PubMed: 11790792]

Hashimoto M, Hsu LJ, Xia Y, Takeda A, Sisk A, Sundsmo M, et al. Oxidative stress induces amyloid-like aggregate formation of NACP/α-synuclein in vitro. Neuroreport. 1999; 10:717–721. [PubMed: 10208537]

Hsu LJ, Sagara Y, Arroyo A, Rockenstein E, Sisk A, Mallory M, et al. Alpha-synuclein promotes mitochondrial deficit and oxidative stress. Am J Pathol. 2000; 157:401–410. [PubMed: 10934145]

Leng Y, Chase TN, Bennett MC. Muscarinic receptor stimulation induces translocation of an alpha-synuclein oligomer from plasma membrane to a light vesicle fraction in cytoplasm. J Biol Chem. 2001; 276:28212–28218. [PubMed: 11337491]

Li W, Lesuisse C, Xu Y, Troncoso JC, Price DL, Lee MK. Stabilization of alpha-synuclein protein with aging and familial Parkinson's disease-linked A53T mutation. J Neurosci. 2004; 24:7400–7409. [PubMed: 15317865]

Linnertz C, Saucier L, Ge D, Cronin KD, Burke JR, Browndyke JN, et al. Genetic regulation of alpha-synuclein mRNA expression in various human brain tissues. PLoS One. 2009; 4:e7480. [PubMed: 19834617]

Lydiatt WM, Denman D, McNeilly DP, Puumula SE, Burke WJ. A randomized, placebo-controlled trial of citalopram for the prevention of major depression during treatment for head and neck cancer. Arch Otolaryngol Head Neck Surg. 2008; 134:528–535. [PubMed: 18490576]

Manning-Bog AB, McCormack AL, Purisai MG, Bolin LM, Di Monte DA. Alpha-synuclein overexpression protects against paraquat-induced neurodegeneration. J Neurosci. 2003; 23:3095–3099. [PubMed: 12716914]

Mar Fan HG, Clemons M, Xu W, Chemerynsky I, Breunis H, Braganza S, et al. A randomized, placebo-controlled, double-blind trial of the effects of d-methylphenidate on fatigue and cognitive dysfunction in women undergoing adjuvant chemotherapy for breast cancer. Support Care Cancer. 2008; 16:577–583. [PubMed: 17972110]

Miaskowski C, Paul SM, Cooper BA, Lee K, Dodd M, West C, et al. Trajectories of fatigue in men with prostate cancer before, during, and after radiation therapy. J Pain Symptom Manage. 2008; 35:632–643. [PubMed: 18358683]

Mitchell SA. Cancer-related fatigue: state of the science. PM &R. 2010; 2:364–383.

Mock V, Atkinson A, Barsevick A, Cella D, Cimprich B, Cleeland C, et al. NCCN practice guidelines for cancer-related fatigue. Oncology. 2000; 14:151–161. [PubMed: 11195408]

Monga U, Kerrigan AJ, Thornby J, Monga TN. Prospective study of fatigue in localized prostate cancer patients undergoing radiotherapy. Radiat Oncol Investig. 1999; 7:178–185.

Monti B, Polazzi E, Batti L, Crochemore C, Virgili M, Contestabile A. Alpha-synuclein protects cerebellar granule neurons against 6-hydroxydopamine-induced death. J Neurochem. 2007; 103:518–530. [PubMed: 17635667]

Musgrove RE, King AE, Dickson TC. Neuroprotective upregulation of endogenous alpha-synuclein precedes ubiquitination in cultured dopaminergic neurons. Neurotox Res. 2011; 19:592–602. [PubMed: 20617407]

Nemani VM, Lu W, Berge V, Nakamura K, Onoa B, Lee MK, et al. Increasing expression of alpha-synuclein reduces neurotransmitter release by inhibiting synaptic reclustering after endocytosis. Neuron. 2010; 65:66–79. [PubMed: 20152114]

Olivares D, Huang X, Branden L, Greig NH, Rogers JT. Physiological and pathological role of alpha-synuclein in Parkinson's disease through iron-mediated oxidative stress; the role of a putative iron-responsive element. Int J Mol Sci. 2009; 10:1226–1260. [PubMed: 19399246]

Piper BF, Dibble SL, Dodd MJ, Weiss MC, Slaughter RE, Paul SM. The revised Piper Fatigue Scale: psychometric evaluation in women with breast cancer. Oncol Nurs Forum. 1998; 25:677–684. [PubMed: 9599351]

Quinn JG, Coulson DT, Brockbank S, Beyer N, Ravid R, Hellemans J, et al. α-Synuclein mRNA and soluble α-synuclein protein levels in post-mortem brain from patients with Parkinson's disease, dementia with Lewy bodies, and Alzheimer's disease. Brain Res. 2012; 1459:71–80. [PubMed: 22560502]

Rönnbäck L, Hansson E. On the potential role of glutamate transport in mental fatigue. J Neuroinflammation. 2004; 1:22. [PubMed: 15527505]

Smets EM, Visser MR, Willems-Groot AF, Garssen B, Oldenburger F, van Tienhoven G. Fatigue and radiotherapy: experience in patients undergoing treatment. Br J Cancer. 1998; 78:899–906. [PubMed: 9764581]

Sulzer D. Clues to how alpha-synuclein damages neurons in Parkinson's disease. Mov Disord. 2010; 25(Suppl 1):S27–31. [PubMed: 20187229]

Thompson I, Thrasher JB, Aus G, Burnett AL, Canby-Haqino ED, Cookson MS, et al. Guideline for the management of clinically localized prostate cancer: 2007 update. J Urol. 2007; 177:2106–2131. [PubMed: 17509297]

Wang XM, Wu TX, Hamza M, Ramsay ES, Wahl SM, Dionne RA. Rofecoxib modulates multiple gene expression pathways in a clinical model of acute inflammatory pain. Pain. 2007; 128:136–147. [PubMed: 17070997]

Westerlund M, Belin AC, Anvret A, Hakansson A, Nissbrandt H, Lind C, et al. Cerebellar alpha-synuclein levels are decreased in Parkinson's disease and do not correlate with SNCA polymorphisms associated with disease in a Swedish material. FASEB J. 2008; 22:3509–3514. [PubMed: 18606870]

Wilker E, Yaffe MB. 14-3-3 proteins – a focus on cancer and human disease. J Mol Cell Cardiol. 2004; 37:633–642. [PubMed: 15350836]

Wratten C, Kilmurray J, Nash S, Seldon M, Hamilton CS, O'Brien PC, et al. Fatigue during breast radiotherapy and its relationship to biological factors. Int J Radiat Oncol Biol Phys. 2004; 59:160–167. [PubMed: 15093912]
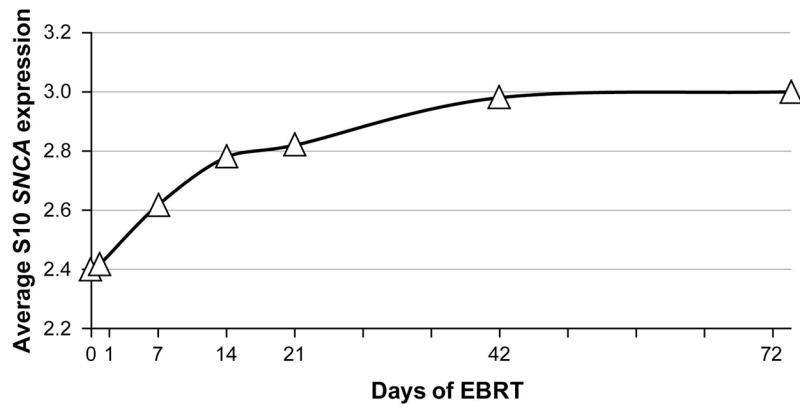
Figure 1. Expression of *SNCA* gene during EBRT by microarray
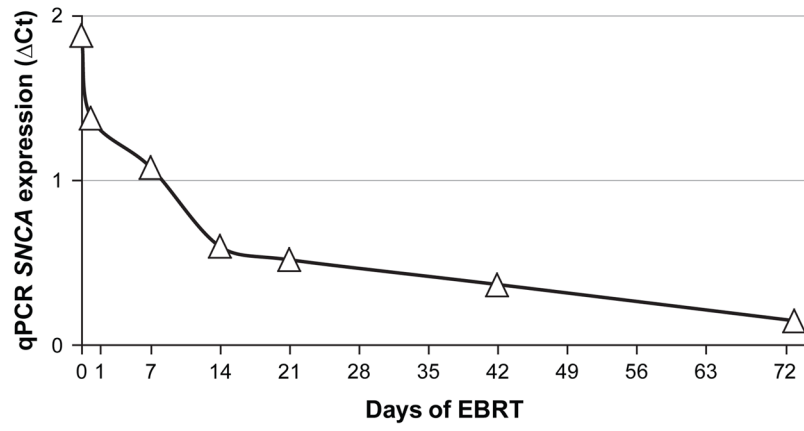*SNCA* = alpha-synuclein gene, EBRT = external beam radiation therapy

Figure 2. *SNCA* **expression during EBRT as confirmed by qPCR**
SNCA = alpha-synuclein gene, EBRT = external beam radiation therapy, ΔCt = delta cycle time (an approximation method), qPCR = quantitative polymerase chain reaction
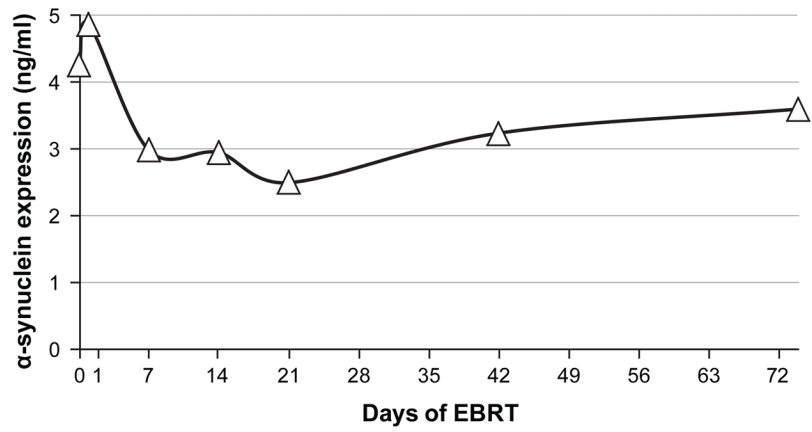
Figure 3. Alpha-synuclein plasma concentration during EBRT
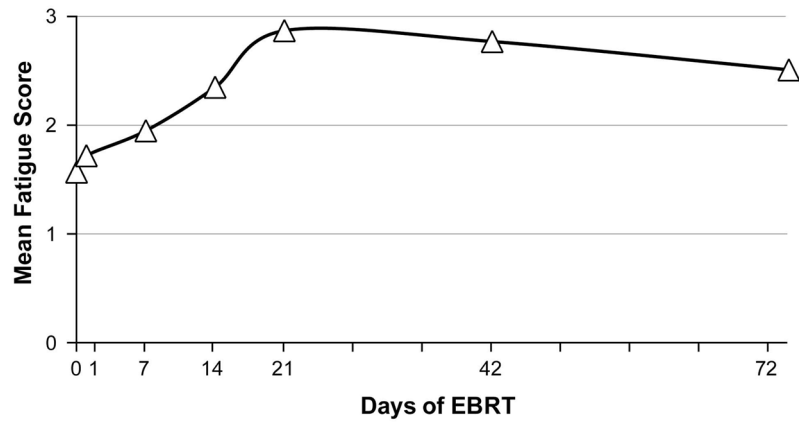ng/ml = nanogram per milliliter, EBRT = external beam radiation therapy

Figure 4. Fatigue scores during EBRT
EBRT = external beam radiation therapy. Fatigue was measured using the revised Piper
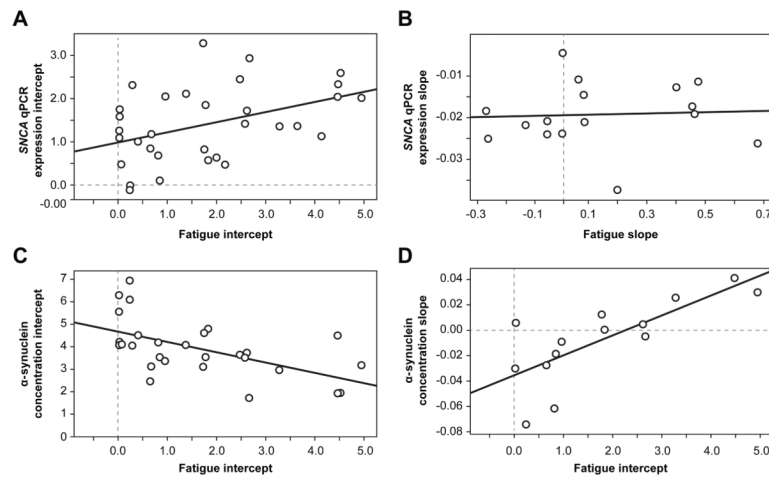Fatigue Scale.

Figure 5. Correlation between fatigue and α-synuclein expression
The changes of fatigue and gene/protein expressions were modeled in a linear fashion. The intercept of the individual growth curve represents the estimated baseline (D0) value for each patient based on a linear trajectory of the values over time during EBRT. The slope of the individual growth curve represents the estimated rate of change over time for each patient based on a linear trajectory of their scores. The intercepts and slopes of fatigue scores were estimated based on mixed model for each patient and the resulting estimated intercepts and slopes were then correlated.
Figure 5a. Correlation between fatigue and *SNCA* **qPCR expression intercepts.**
SNCA = alpha-synuclein gene; qPCR = quantitative polymerase chain reaction
Figure 5b. Correlation between fatigue and *SNCA* **qPCR expression slopes.**
SNCA = alpha-synuclein gene; qPCR = quantitative polymerase chain reaction
Figure 5c. Correlation between fatigue and α-synuclein protein intercepts.
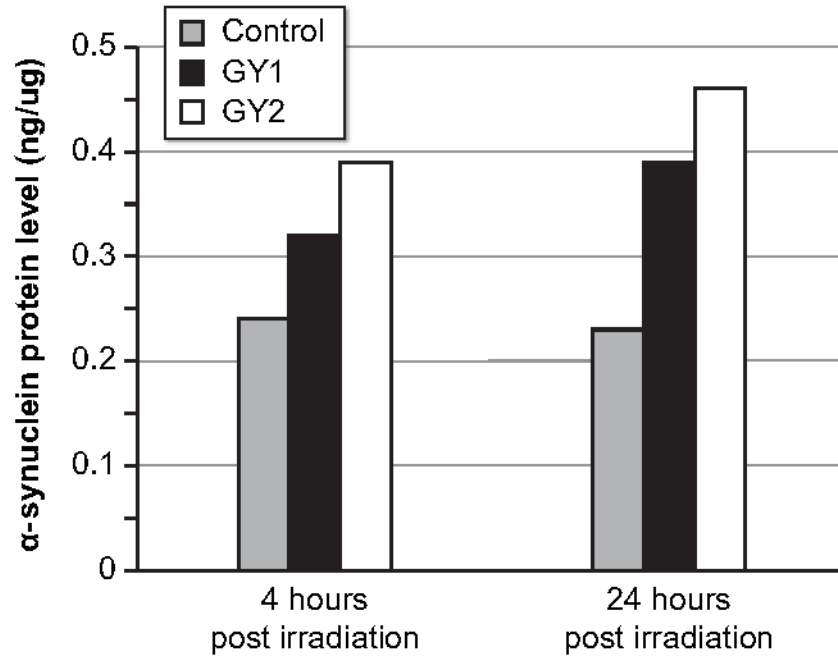Figure 5d. Correlation between fatigue intercept and α-synuclein protein slope.

Figure 6. Effect of prostate cell irradiation on α-synuclein expression
ng = nanogram, ml = milliliter, two doses of radiation used = 1 Gray (GY1) and 2 Gray (GY2)

Table 1

Top 20 Differentially expressed genes by microarray.

Upregulated Genes			Downregulated Genes		
Genes Symbol	Gene Name	Expression Value	Genes Symbol	Gene Name	Expression Value
IFI27	Interferon alpha-inducible protein 27	0.774	*MS4A1*	B-lymphocyte antigen CD20	−0.821
CA1	Carbonic anhydrase 1	0.705	*IGHM*	Ig mu chain C region	−0.816
HBD	Hemoglobin subunit delta	0.640	*PAX5*	Paired box protein Pax-5	−0.791
XK	X-linked Kx blood group	0.534	*FCRLA*	Fc receptor-like A	−0.669
HBG2	Hemoglobin subunit gamma-2	0.513	*TTC3*	Tetratricopeptide repeat protein 3	−0.647
RHCE/RHD	Blood group Rh(CE) polypeptide	0.507	*NSUN5C*	NOP2/Sun domain family, member 5C	−0.642
AHSP	Alpha hemoglobin stabilizing protein	0.496	*POU2AF1*	POU domain class 2- associating factor 1	−0.636
GYPB	Glycophorin B	0.483	*CCR7*	C-C chemokine receptor type 7	−0.632
SNCA	**Alpha synuclein**	**0.470**	*FAIM3*	Fas apoptotic inhibitory molecule 3	−0.613
ISCA1	Iron-sulfur cluster assembly 1 homolog	0.464	*BLK*	B lymphoid tyrosine kinase	−0.612

Table 2

Clinical and demographic characteristics of the samples.

Characteristics	Subjects- Baseline (n=16)	Subjects- Completion (n=16)	Controls (n=16)	Normal Range
Age (in years), mean (range)	63 (49–81)		58 (43–84)	
Race, n (%)				
Caucasian	10 (63.0)		10 (63.0)	
African American	2 (12.0)		2 (12.0)	
Others	4 (25.0)		4 (25.0)	
Body Mass Index, mean (SD)	30.4 (5.0)		27.8 (2.7)	
Testosterone, mean (SD)	211.3 (178.8)			181.0–758.0 ng/dL
Thyroid Stimulating Hormone, mean (SD)	1.8 (1.1)		2.0 (1.7)	0.4–4.0 μIU/mL
Albumin, mean (SD)	4.1 (0.3)		4.0 (0.3)	3.7–4.7 g/dL
Depression, mean (SD)	1.4 (2.5)	2.0 (2.7)	0.5 (0.3)	
Hematocrit, mean (SD)	40.9 (3.4)	37.8 (2.8)	44.2 (3.2)	40.1–51.0%
Prostate Specific Antigen, mean (SD)	21.0 (27.6)	0.1 (0.3)		0.0–4.0 μg/L
Clinical T Stage, n (%)				
T1c	2 (12.0)			
T2a	5 (31.0)			
T2b	2 (13.0)			
T2c	3 (19.0)			
T3a	2 (13.0)			
T3b	1 (6.0)			
T3c	1 (6.0)			
Gleason Score, n (%)				
6	2 (12.0)			
7	5 (31.0)			
8	3 (19.0)			
9	6 (38.0)			
Karnofsky Score, mean (SD)	89.4 (2.2)			